# Orbital Effects on Pitch Angle Diffusion of Injected Fast-Ion Beams in Tokamaks

by

Joseph J. Wleklinski

B.Sc. Mechanical Engineering
University of Notre Dame, 1997

SUBMITTED TO THE DEPARTMENT OF MECHAINCAL ENGINEERING IN PARTIAL FULFILLMENT OF THE REQUIREMENTS FOR THE DEGREE OF

MASTER OF SCIENCE IN MECHANICAL ENGINEERING
AT THE
MASSACHUSETTS INSTITUTE OF TECHNOLOGY

FEBRUARY 2005



Signature of Author:_____
Department of Mechanical Engineering
January 14th, 2005

Certified by:_____
Jan Egedal
Research Scientist, Plasma Science Fusion Center
Thesis Supervisor

Certified by:_____
Ain Sonin
Professor of Mechanical Engineering

Accepted by:_____
Lallit Anand
Professor of Mechanical Engineering
Chair, Graduate Committee

Orbital Effects on Pitch Angle Diffusion
of Injected Fast-Ion Beams in Tokamaks

by

Joseph J. Wleklinski

Submitted to the Department of Mechanical Engineering
On January 14th, 2005 in Partial Fulfillment of the
Requirement for the Degree of Master of Science in
Mechanical Engineering

ABSTRACT

The effects of ion orbits on pitch angle scattering of fast ion beam injection are investigated here for the magnetic equilibrium of the ITER tokamak. Two methods are used to calculate distributions in the presence of orbits, one applying boundary conditions a posteriori and one a priori. In both cases an orbit average of the Fokker-Planck equation is taken, yielding a solution in velocity space variables velocity and pitch angle. In the first case, conditions in the form of a linear combination of co, counter, and trapped distributions or fluxes are matched at the orbit transition value of pitch angle so that several distributions combine to form a solution. In the second case, an overall distribution is found which obeys boundary conditions derived from the trapped and passing regime essential behavior. Ultimately, both methods yield distributions which are essentially equivalent in character.

Thesis Supervisor: Jan Egedal
Title: Research Scientist, Plasma Science Fusion Center

INTRODUCTION

First we will present the basic theory underlying orbital motion in a tokamak and then describe the orbital effect on the velocity diffusion of injected fast ions.

In a magnetic field charged particles obey the Lorenz force law

$$\mathbf{F} = q\mathbf{v} \times \mathbf{B}$$

The particles are free to move along a magnetic field line with parallel velocity $v_{//} = |\mathbf{v}\ \mathbf{B}|/B$ and also gyrate around magnetic field lines with a frequency $\omega_c = qB/m$ known as the gyrofrequency and with a radius of $\rho_l = mv/(qB)$ known as the Larmor radius. The center of gyration at any instant is known as the guiding center. In a stationary, homogeneous magnetic field the guiding center trajectories coincide with the field lines, but in general this is not the case. For analysis of particle trajectories in more complicated cases it is useful to introduce constants of motion.

In the Lorentz force law the force exerted by a magnetic field on a charged particle is perpendicular to its motion; thus magnetic fields do no work and the energy of a particle ($E=mv^2/2$, ignoring electrostatic potential energy) is a constant of the motion. Another constant of the motion is the magnetic moment $\mu = mv^2/2B$. For periodic or nearly periodic motion the action variable in classical mechanics is an adiabatic invariant

$$J = \oint p dq$$

Here $p$ and $q$ are canonical momentum and position. For gyration about a guiding center,

$$J = \oint m v_{\perp} ds = \frac{4\pi m}{q} \mu$$

Combining these two constants of motion into one expression results in the definition of the principle of reflection.

$$v_{//}^2 = \frac{2(E - B\mu)}{m}$$

A particle traveling in an inhomogeneous field may experience an increasing $B$ as a function of time. When $B\mu$ approaches $E$, $v_{//}$ vanishes and then reverses sign; the particle is reflected in a "magnetic mirror."

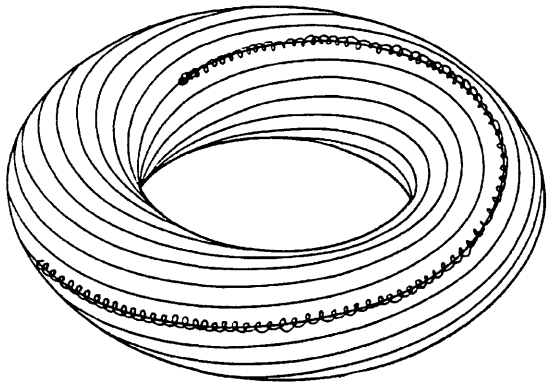

Figure 1. Field lines and a typical orbit (path shown with gyrations) on a toroidal tokamak flux surface

In a tokamak, magnetic field lines on a flux surface circulate about a torus as shown in Figure 1, in a closed toroidal magnetic configuration. The field lines also have a helical twist due to the poloidal magnetic field of the plasma current. Poloidal flux surfaces, surfaces of constant magnetic flux are defined by

$$\psi = \int_0^R R' B_\theta dR'$$

Where $R$ is the major axis of the torus, $B_\theta$ the poloidal magnetic field. Particles orbit approximately along the magnetic flux surfaces with deviation due to curvature and grad $B$ drifts, which are a drifting of a particle from its path due to changes in the curvature of the magnetic field and to gradient of the magnetic field along its path, repectively. There are three main types of orbits in a tokamak: co- and counter-going orbits, and trapped orbits, shown in the poloidal cross sections of Figure 2. Trapped orbits are those with a reflection. Co-going orbits encircle the torus in the direction of the plasma current density $J$, and counter-going are those for in the opposite direction of the current density $J$. At the position of greatest magnitude along the major radius, the relative values of $\mathbf{v_B} = v_{//}\mathbf{B}/|\mathbf{B}|$ and $\mathbf{v_d}$ (the drift velocity) determine the character of the orbits. As in Figure 2, trapped orbits have a banana shape with a small finite banana width and two reflection points defining the average flux surface.

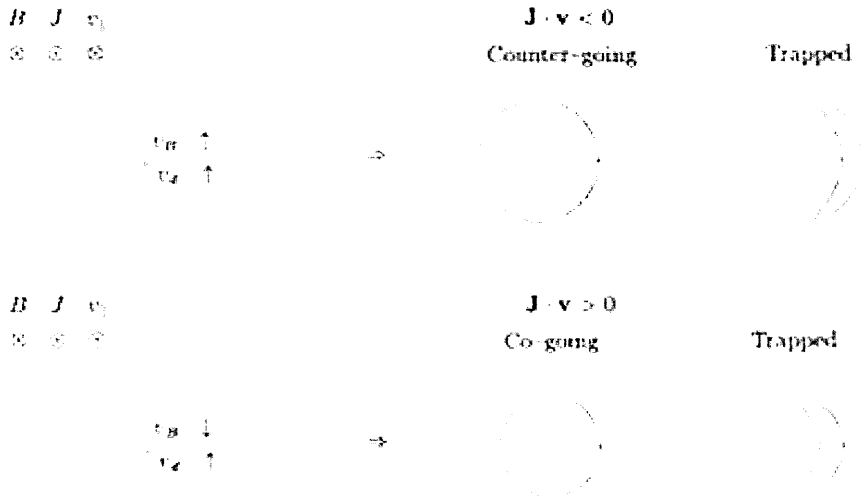


Figure 2. Four possible tokamak orbits for different orientations of magnetic field, toroidal current, and velocity. The relative directions of velocity parallel to the magnetic field and the drift velocity determine the orbit characteristics.

A third constant of the motion is the toroidal canonical angular momentum, $p_\phi$:

$$p_\phi = dL/d\dot{\phi}$$

where $L$ is the Lagarangian,

$$L = \frac{1}{2}mv^2 + q\mathbf{A}\cdot\mathbf{v}$$

$\phi$ is the toroidal angular coordinate and **A** the magnetic vector potential. If the pitch angle is defined with

$$v_\phi = R\dot{\phi} = v\zeta\frac{B_\phi}{B}$$

where $\zeta = v_{//}/v$, we then arrive at an equation important for describing orbits in a tokamak:

$$p_\phi = q\psi - \chi Rmv\frac{B_\phi}{B}$$

$p_\phi$has the significance of being the average flux surface times the particle charge, and thus, as stated above, trapped orbits have the property that when $\mathbf{v}_{//}$=0, $q\psi = p_\phi$. The phase space variables used here will be velocity $v$ and pitch angle $\zeta = v_{//}./\mathrm{v}$. As the phase is adjusted, the poloidal shapes of the orbits change and orbit transition can occur. When a trapped orbit's bounce points meet, transition can occur from trapped to co, from trapped to counter, or from trapped back to trapped. A detailed analysis of orbit topology is given in [1]. A property of an orbit is its bounce time, $\tau_b$, the time it takes to complete a full drift orbit. At the transition point the bounce time becomes infinite.

In neutral beam heating of plasma in a tokamak, neutral injected particles are ionized and slowed by Coulomb collisions with an equilibrium Maxwellian background of ions and electrons, a diffusion process in the phase space. Namely, in pitch angle and velocity the distribution diffuses monotonically from some initial value to some minimum value at its bounds. The pitch angle diffusion of fast ion injection is a well known process [3], but it has heretofore been considered by Cordey [2] outside of the

context of the orbits the ions assume after injection. We improve upon Cordey's analysis by applying it to ITER tokamak magnetic field data with a correction term in the order of the Legendre solutions derived from boundary conditions. A complete explanation of this is given later. The neutral beam atoms can penetrate the flux surfaces, but as soon as they become ionized they immediately begin to orbit the magnetic field with the rest of the plasma. Since orbits are a function of pitch angle, orbiting enhances the diffusion significantly (as will be shown), manifested by a more spread distribution and greater flux in phase space, especially in the trapped region. A critical complication occurs at the transition point. Flux in phase space can go between all types of orbits. A significant result is that the distribution and its derivative with respect to pitch angle is continuous at the transition boundary. It is hoped that this paper serves as a basis for more complete future treatment of diffusion from a fast ion injection source.

## THEORY

The standard relaxation to thermal energy is described by the Fokker-Planck equation in the two dimensional velocity space variables velocity $v$ and pitch angle $\zeta$ [5]:

$$\frac{1}{v^2}\frac{\partial}{\partial v}\left[\left(v^3+v_C^3\right)f\right]+\beta\frac{v_C^3}{v^3}\frac{\partial}{\partial\zeta}\left(1-\zeta^2\right)\frac{\partial f}{\partial\zeta} = -\frac{S\tau_S}{4\pi v^2}\delta(v-v_o)\delta(\zeta-\zeta_o) \tag{1}$$

$D$, $\sigma$, $\nu_c$, and $\beta$, are functions of the plasma parameters that describe Coulomb scattering processes, $S$ is the source strength, $\tau_s$ is the Spitzer time, and $v_o$ and $\zeta_o$ are the source velocity and initial pitch. The term on the right hand side represents the source term. It is in the form of Dirac delta functions such that the solution will be a Green's function of the right-hand-side operator. Orbit averaging (1) reduces the number independent variables from three in $v$, $\psi_f$ and $\zeta$ to $v$ and $\zeta$. $v$ and $\psi_f$ are constant along the orbits. In addition, orbit averaging captures the effects that orbits have on the distribution. We subject (1) to orbit averaging by multiplying by $ds/v_{//}$, integrating and normalizing by the integral of $1/(ds/v_{//})$, the bounce time. The solution for a cylindrical plasma before orbit averaging away from the source is well known [5], [3] and has the form

$$f(v,\zeta)=\frac{S\tau_S}{v^3+v_C^3}\sum_{n=0}^{\infty}\left(n+\frac{1}{2}\right)u^{n(n+1)}P_n(\zeta_o)P_n(\zeta) \tag{2}$$

where $P_n$ is the $n^{th}$ Legendre polynomial, and

$$u=\left(\frac{v_o^3+v_C^3}{v^3+v_C^3}\frac{v^3}{v_o^3}\right)^{\beta/3}$$

Another solution valid near the source ($v$=$v_o$) has more recently been evaluated [5] and has the form

$$f(v,\zeta)=\frac{S\tau_S}{v^3+v_C^3}\frac{\exp\left(-\frac{(\zeta-\zeta_o)^2}{4\alpha}\right)}{2\sqrt{\pi\alpha}}$$

where

$$\alpha=\frac{\pm\beta\left(1-\zeta_o^2\right)}{3}\ln\left(\frac{1+(v_C/v)^3}{1+(v_C/v_o)^3}\right)$$

We make use of the former solution because we are interested in large scale variation in velocity. After orbit averaging we retain the same form of solution with a change of variable from $\zeta$ to a function of pitch angle $g(\lambda)$ where $\lambda = \mu/E$. To arrive at this, we first take an orbit average of the second term in (1). Then we fashion it as such:

$$\frac{1}{\tau_b}\oint\frac{ds}{v_{//}}\beta\frac{v_C^3}{v^3}\frac{\partial}{\partial\zeta}\left(1-\zeta^2\right)\frac{\partial f}{\partial\zeta}=\beta\frac{v_C^3}{v^3}\frac{\partial}{\partial g}\left(1-g^2\right)\frac{\partial f}{\partial g}$$

$$\zeta=v\sqrt{1-B\lambda};\quad g=g(\lambda) \tag{3}$$

in $\lambda$ space, where $B$ is the magnetic field. Orbit averaging the first term of equation (1) results in the same term since $v$ is a constant of motion. Orbit averaging the right-hand side just results in the change of variable from $\zeta$ to $\lambda$ taking effect. The solution becomes,

$$f(v,g)=\frac{S\tau_S}{v^3+v_C^3}\sum_{n=0}^{\infty}\left(n+\frac{1}{2}\right)\mu^{n(n+1)}P_n(g_o)P_n(g) \tag{4}$$

where

$$g_o = g(\lambda_o)$$

and $\lambda_o$ is the injection pitch angle. We can make use of the comparison of (3) in independent variable $g$ to its orbit average in independent variable $\lambda$. First, we expand the form for the last term in (3) in terms of $g(\lambda)$ to find an expression for in derivatives of $\lambda$:

$$\frac{\partial}{\partial g}\left(1-g^2\right)\frac{\partial f}{\partial g}=\left(\frac{g''-2gg'}{g'^2}\right)\frac{\partial f}{\partial \lambda}+\left(\frac{1-g^2}{g'^2}\right)\frac{\partial^2 f}{\partial \lambda^2} \tag{5}$$

Then we calculate the orbit average of the second term of (1), expand in derivatives of $\lambda$, and compare to coefficients of the above:

$$\oint\frac{ds}{v_{//}}\frac{\partial}{\partial\zeta}\left(1-\zeta^2\right)\frac{\partial f}{\partial\zeta}$$

$$=\frac{1}{\tau_b}\oint\frac{ds}{v_{//}}\frac{\sqrt{1-B\lambda}}{B}\left(\sqrt{1-B\lambda}\,\frac{\partial f}{\partial\lambda}-\frac{\lambda B}{2\sqrt{1-B\lambda}}\frac{\partial f}{\partial\lambda}+\lambda\sqrt{1-B\lambda}\,\frac{\partial^2 f}{\partial\lambda^2}\right)$$

$$=\frac{4}{\tau_b}\oint\frac{ds}{v_{//}}\left[\left(\frac{1-B\lambda}{B}-\frac{\lambda}{2}\right)\frac{\partial f}{\partial\lambda}+\frac{\lambda}{B}\left(1-B\lambda\right)\frac{\partial^2 f}{\partial\lambda^2}\right] \tag{6}$$

$$=\left(4\langle 1/B\rangle-6\lambda\right)\frac{\partial f}{\partial\lambda}+\left(4\lambda\langle 1/B\rangle-4\lambda^2\right)\frac{\partial^2 f}{\partial\lambda^2}=C\frac{\partial f}{\partial\lambda}+D\frac{\partial^2 f}{\partial\lambda^2}$$

We find

$$\frac{(1-g^2)}{g'^2} = D$$

$$-\frac{(2gg'-g'')}{g'^2} = C$$

In solving these equations for $g$ we want to solve no differential equations since boundary equations are unclear. We first differentiate $D$, then substitute for $D$ and $D$' and $C$ in (6) After algebra

$$(2C(\lambda)g(\lambda)+C'(\lambda))\sqrt{\frac{1-g(\lambda)^2}{C(\lambda)}} = D(\lambda)C(\lambda)+2g(\lambda)$$

Solving this numerically we find $g$ is continuous at the transition line and monotonically increasing in $\lambda$. Continuity is expected because the distribution must be continuous as a result of fast diffusion, which will be explained below. $g$ is also expected to be monotonically increasing in $\lambda$ because the flux must always be negative going away from the injection source in $\lambda$, also a characteristic of a diffusive process. In figure 3 we plot $g$ against the fit

$$g(\lambda) = \tanh(15(\lambda - .128)) \tag{7}$$

and see that it obeys quite well. A required property is that |g| always be less than 1. The property that when the argument of tanh is negative, $g$-> -$g$ will be useful in the next section, and in fact the Legendre operator in (1) is the same for $g$ or $-g$.

Complication arises in $f$ when the pitch angle becomes critical at the orbit transition value. The sources emanating form the transition line do so according to (4) applied continuously at each point along the line. The source strength coefficient is proportional to the flux of the original source evaluated at the transition line plus the flux of each transition source of higher velocity into the boundary. This latter contribution to the source strength is the result of velocity diffusion down the transition line. The sources are expressed as:

$$f(v,g)=\frac{S\tau_S}{v^3+v_C^3}\sum_{n=0}^{\infty}\left(n+\frac{1}{2}\right)u^{n(n+1)}P_n(g_t)P_n(g)$$

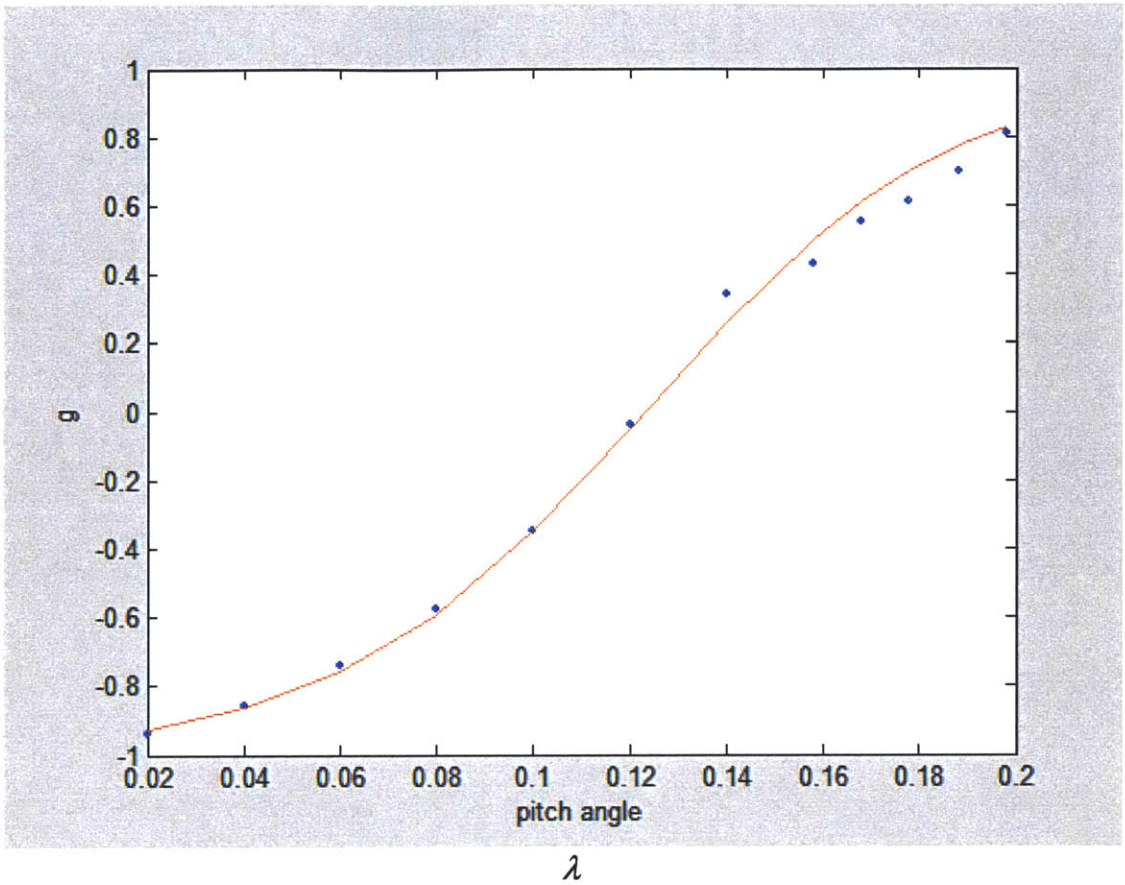


Figure 3. Mapping function g($\lambda$).

where

$$S = \left.\frac{df_1}{d\lambda}\right|_{\lambda=\lambda_t, v=v_m} + \sum_{n=1}^{m-1} \left.\frac{df_n}{d\lambda}\right|_{\lambda=\lambda_t, v=v_m}$$

Here the first term in $S$ is the flux of the injected ions at a particular velocity $v_m$ along the transition line. The second term is the flux at $v_m$ of all co, counter and trapped distributions flowing from the transition line which are above $v_m$. $m$ refers to the velocity coordinate along the transition line of the source, while $n$ are the velocity coordinates above $m$ on the transition line. $\Sigma\, df_n/d\lambda$ is the flux of all three transition distributions.

At this point we just express $S$ as proportional to these fluxes; however, the relative magnitudes of the original flux and the transition flux are the same, i.e., the coefficients of each are unity. This is because each comes from fluxes which are directly comparable to eachother. In fact the original source can be considered as flowing into a sink at the transition line which then becomes a source of transition flux. This will be shown below.

Also at the transition line, the flux is continuous, and each type of orbit's distribution is equal. The latter is a result of the fast diffusion assumption that diffusion rate is much faster than the rate of transition. As the orbits split from co to co, counter and trapped, the equality of types of overall distributions is expressed as:

$$f_1 = f_{-1} = f_o \mid_{\lambda=\lambda_c} \tag{8}$$

Also, the weighted velocity fluxes at the transition line are equal

$$\sum_n A_n \frac{df}{d\lambda} \mid_{\lambda=\lambda_c} = 0 \tag{9}$$

where $A_n$ are weight functions of velocity. Trapped orbits have a relative flux double that of the others because trapped orbits interface with co and with counter orbits at the transition line. There are four individual distributions, $f_{1a}$, $f_1$, $f_{-1}$, and $f$, which are the original source (co), and three sources (co, counter and trapped) originating from the transition line. As mentioned above the transition sources act as a sink to which the original source flows. As a result of (6) and (7), these four distributions are related by the following:

$$f_{1a} + A(v) f_1 = B(v) f_o = C(v) f_{-1} \tag{10}$$

$$\frac{df_{1a}}{d\lambda} = A(v)\frac{df_{sa}}{d\lambda} + B(v)\frac{df_{sa}}{d\lambda} + C(v)\frac{df_{sa}}{d\lambda} \tag{11}$$

The coefficients are determined such that both of (8)-(9) are fulfilled, yielding

$$f_{1s} + (A(v) + 2B(v)) f_{1-s} + A(v) f_1 = B(v) f_{-1} = C(v) f_o \Big|_{\lambda=\lambda_c} \tag{12}$$

## SOLUTION VIA SELECTED EIGENFUNCTIONS AS DETERMINED BY BOUNDARY CONDITIONS

A second way to obtain a solution is to impose boundary conditions before the eigenfunctions are determined. This was done by Cordey [2] which, applied to the ITER magnetic field data, involves using the minimum magnetic field value for the given average magnetic flux surface on which the orbit lies to define the independent variable $\chi$:

$$\chi = \sqrt{1 - \lambda B_{\min}}$$

The analysis consists of the following operator, eigenfunctions $C_n$, and boundary

conditions all to first order in trapped fraction $\varepsilon$.

$$\frac{d}{d\chi}\left(1-\chi^2\right)\frac{dC_n}{d\chi}+\alpha_n C_n=0$$

$$f=\sum a_n(v)C_n(\chi) \qquad (11)$$

$C_n$ *continuous at* $\chi=\pm\chi_{transitio}$

$$\left.\frac{\partial C_n}{\partial\chi}\right|_{\chi_t^-}-\left.\frac{\partial C_n}{\partial\chi}\right|_{-\chi_t^-}=2\left.\frac{\partial C_n}{\partial\chi}\right|_{\chi_t^-}$$

$$C_n(-\chi)=C_n(\chi)\ ,\ \chi_t<\chi<\chi_t \qquad (12)\text{-}(15)$$

$C_n$ *finite at* $\chi=\pm1,0$

The last condition implies that the eigenfunctions for negative pitch angle are equal to the eigenfunction for positive pitch angle times a constant.

$$C_n(-\chi)=AC_n(\chi) \qquad (16)$$

The penultimate condition (14) imposes the eigenfunctions are equal at the transition points.

$$C_n(-\chi_t)=C_n(\chi_t) \qquad (17)$$

(16) and (17) imply that

$$A=1 \quad or \quad C_n(\pm\chi_t)=0 \tag{18}$$

These two conditions lead to two sets of orthogonal eigenfunctions, one even in $\chi$ and one odd in $\chi$. The odd eigenfunctions vanish at $\chi_t$ and satisfy (23 here). The solutions are Legendre functions of order given by

$$P_n(\pm\chi_t)=0 \tag{19}$$

Using a Taylor expansion of Legendre polynomials of integer order, (19) can be put in terms of integer order Legendre functions and the derivatives of Legendre functions with respect to the order:

$$P_{\nu_n}=P_n(\chi_t)+(\nu_n-n)\frac{\partial P_n(\chi_t)}{\partial n} \tag{20}$$

The condition on odd eigenfunctions is then

$$P_n(\chi_t)+(\nu_n-n)\frac{\partial P_n(\chi_t)}{\partial n}=0 \tag{21}$$

and for $-\chi_t<\chi<\chi_t$, To satisfy continuity of the eigenfunctions and the flux, $C_n$ must be zero in the trapped region . Cordey gives an approximate value of $\nu_n$ in (20a) for $n$ odd

to satisfy the boundary condition (21):

$$\nu_n = n + \frac{4\lambda_t}{\pi} \frac{\Gamma^2(1+n/2)}{\Gamma^2((1+n)/2)} \tag{21}$$

Equation (20) is still not exact using the above order. To make it more accurate, here we improve upon Cordey's method by adding an extra term $L_n(n)$ calculated numerically to satisfy (20) for the ITER data for correction.

The even eigenfunctions are also determined by solving (11), but by then matching at boundaries with boundary conditions (12) (13), This matching defines the order of the eigenfunctions as with the odd:

$$\left(P_n'(\chi_t)+(\nu_n-n)\frac{\partial P_n'(\chi_t)}{\partial n}\right)\Bigg|_{\chi^+} - \left(P_n'(-\chi_t)+(\nu_n-n)\frac{\partial P_n'(-\chi_t)}{\partial n}\right)\Bigg|_{-\chi^-} = 2\left(P_n'(\chi_t)+(\nu_n-n)\frac{\partial P_n'(\chi_t)}{\partial n}\right)\Bigg|_{\chi^-} \tag{22}$$

Where $P'$ is the derivative with respect to $\chi$. This second boundary condition states that the untrapped fluxes at each boundary are equal in magnitude and opposite in sign to the trapped (transition) fluxes. Cordey obtains the orders of these even eigenfunctions approximately to be

$$\nu_n = n + \frac{n(n+1)\lambda_t}{2\pi}\frac{\Gamma^2((1+n)/2)}{\Gamma^2(1+n/2)} \tag{23}$$

The continuity of the even eigenfunctions and flux are automatically satisfied so no correction term is employed. Summarized, the eigenfunctions are

$$C_n = \begin{cases} P_n(\chi) + \chi_t(R_n + L_n)\left.\dfrac{\partial P_\upsilon(\chi)}{\partial \upsilon}\right|_{\upsilon=n} & , \ |\chi| > \chi_t \\ 0 & , \ |\chi| > \chi_t \quad n \ odd \\ P_n(\chi) + \chi_t(R_n + L_n)\left.\dfrac{\partial P_\upsilon(\chi)}{\partial \upsilon}\right|_{\upsilon=n} & , \ |\chi| > \chi_t \quad n \ even \end{cases}$$

. The general solution for beam injection by Cordey reads

$$f = \sum_n K_n C_n t^{n(n+1)\beta^3}(1 + \chi_t(R_n + L_n)(1 + (2n+1)\beta \log t))$$

## RESULTS AND DISCUSSION

This method and the previous are two physically equivalent descriptions of diffusion in the presence of orbits. The two methods share the same features in all three

regions. In the trapped region a concavity exists because flux enters from both boundaries. In the counter orbit region there is some appreciable flux as the distribution recedes with decreasing $\chi$. In figure 4 there is more flux at higher velocities than in figure 5 likely owing to the "backdiffusion" at the transition line as part of the calculation in the previous section for figure 5, to the a posteriori applied boundary conditions, and to more discretization in figure 4. The distribution is correspondingly smaller in the trapped region of the contour plot in figure 4 so that the larger concavity to the flux there is a red herring. The second method is likely more accurate due to more efficient usage of discretization in the employment of boundary conditions, but the first, by introducing "sources" and by using direct orbit averaging of the model equations, might be more useful conceptually or in other diffusion problems.

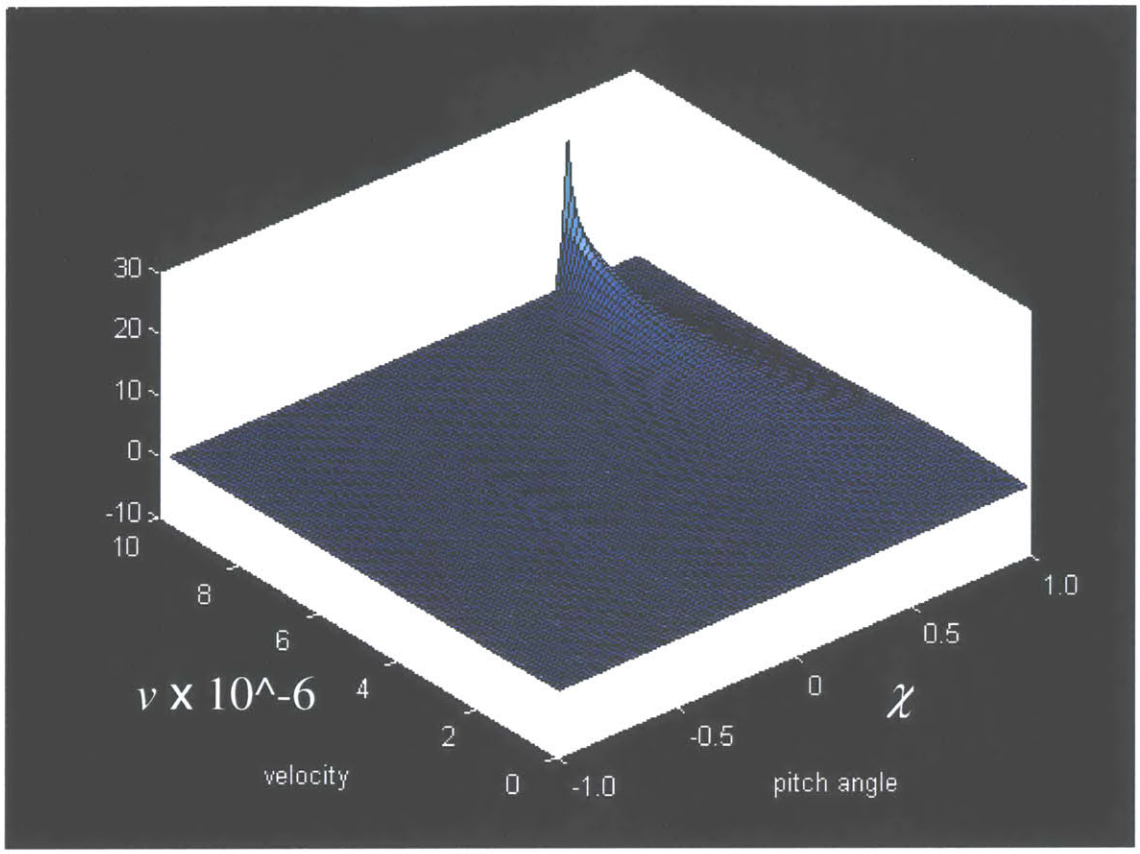


Figure 4. Distribution for fast ion beam injection derived from orthogonal eigenfunctions.

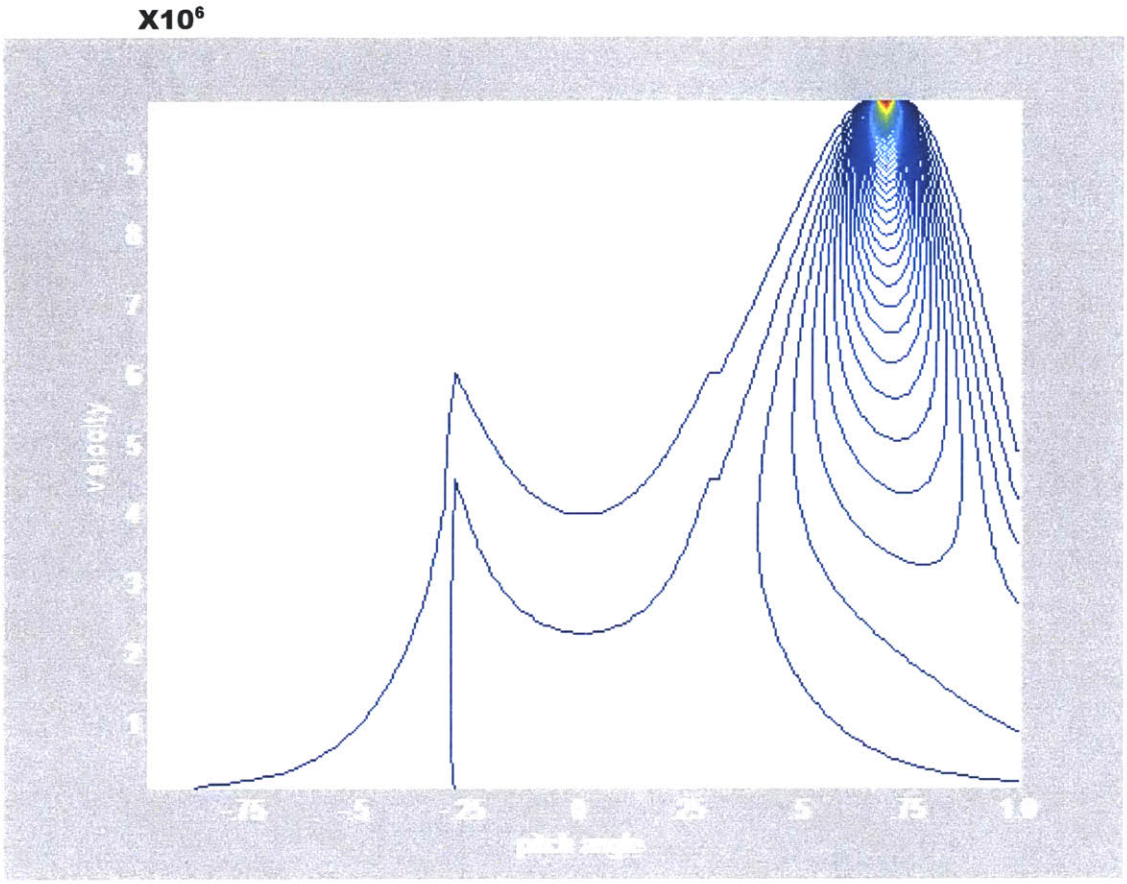


Figure 4b. Contour plot of Figure 3 data.

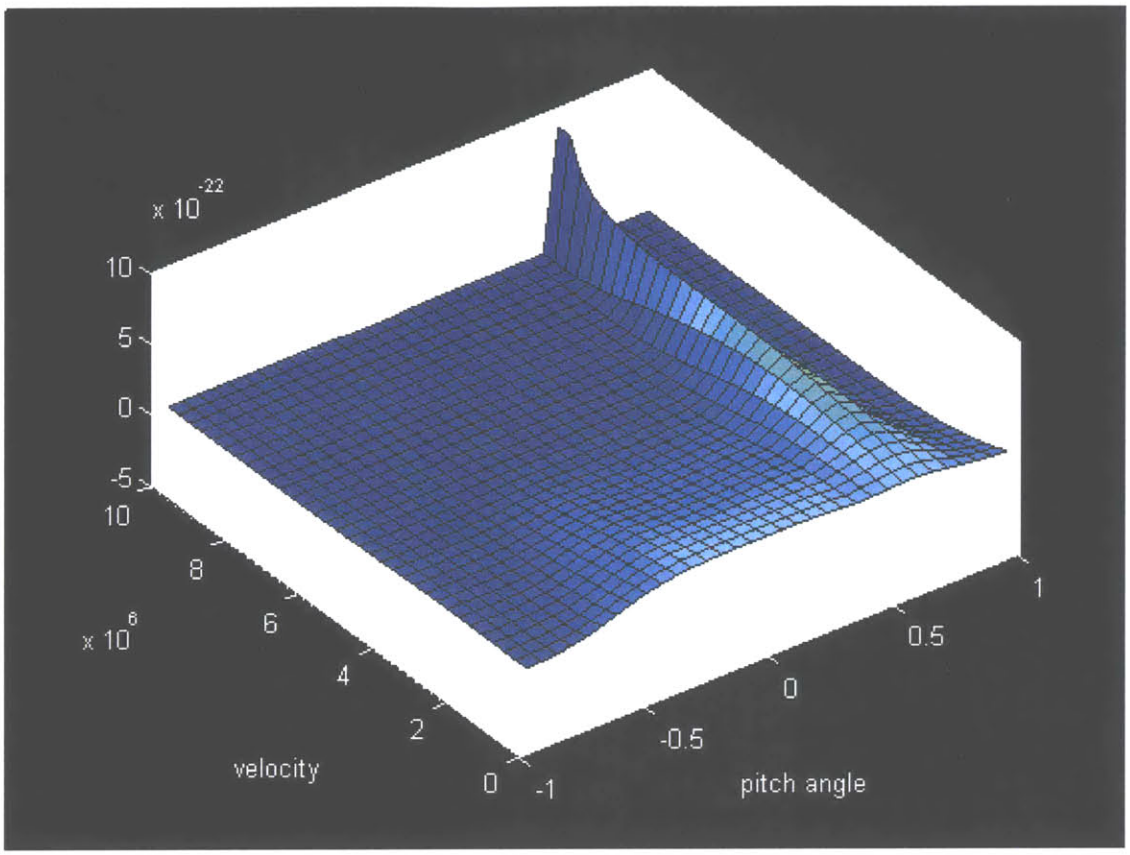


Figure 5. Distribution derived from orbit orbit-averaging of the Fokker-Planck equation and a posteriori application of boundary conditions.

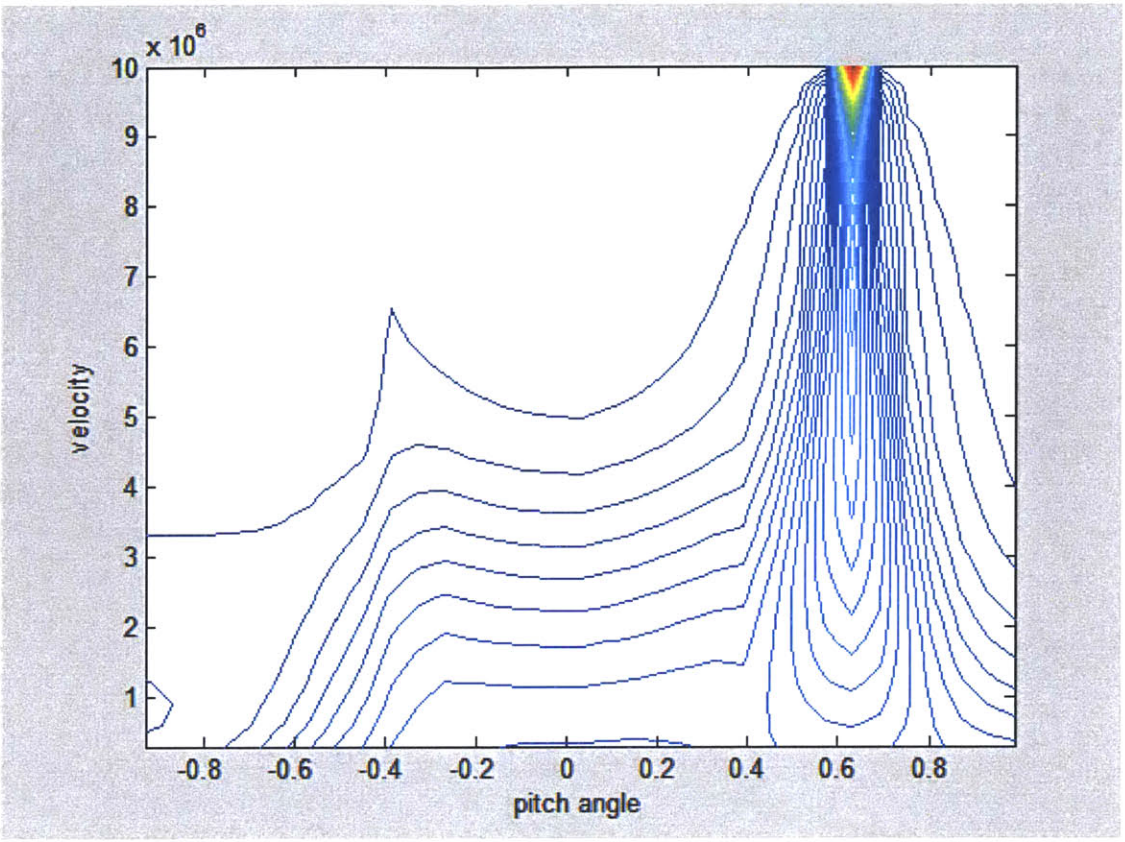


Figure 5b. Contour plot of Figure 4 data.

REFERENCES


1. Egedal, J. "Fast Ions in Tokamaks and their Measurement by Collective Thomson Scattering." PhD thesis, Oxford University (1998).
2. Cordey, J. G. *Nuclear Fusion*. 6, 499 (1976)
3. Cordey, J. G., Core, W. G. F., *Phys. Fluids* 17, 1626 (1974).
4. Egedal, J., "The Orbit Averaged Particle Source from Neutral Beam Injection in Tokamaks," submitted to *Nuclear Fusion* (2005).
5. Core, W. G. F., *Nuclear Fusion*. 33, 829 (1993).